THE ASTROPHYSICAL JOURNAL, 481:973–977, 1997 June 1

ON THE SUBPHOTOSPHERIC ORIGIN OF CORONAL ELECTRIC CURRENTS

ALEXEI A. PEVTSOV AND RICHARD C. CANFIELD
Department of Physics, Montana State University, Bozeman, MT 59717; pevtsov@physics.montana.edu
AND
ALEXANDER N. MCCLYMONT
Institute for Astronomy, University of Hawaii, 2680 Woodlawn Drive, Honolulu, HI 96822; mcclymon@ifa.hawaii.edu
Received 1996 May 3; accepted 1996 December 24

ABSTRACT

Using photospheric vector magnetograms from the Haleakala Stokes Polarimeter and coronal X-ray images from the *Yohkoh* Soft X-Ray Telescope (SXT), we infer values of the force-free field parameter α at both photospheric and coronal levels within 140 active regions. We determine the value of α for a linear force-free field that best fits each magnetogram in a least-squares sense. We average values from all available magnetograms to obtain a single mean photospheric α-value $\langle \alpha_p \rangle$ for each active region. From the SXT images we estimate α in the corona by determining $(\pi/L) \sin \gamma$ for individual loops, where γ is the observed shear angle of X-ray loops of length L. We then average these values of α to obtain a single coronal α value, $\langle \alpha_c \rangle$, for each active region.

In active regions for which the photospheric α-map is predominantly of one sign, we find that the values of $\langle \alpha_p \rangle$ and $\langle \alpha_c \rangle$ are well correlated. Only for active regions in which both signs of α are well represented, and in which our method of analysis therefore breaks down, are the values of $\langle \alpha_p \rangle$ and $\langle \alpha_c \rangle$ poorly correlated. The former correlation implies that coronal electric currents typically extend down to at least the photosphere. However, other studies imply subphotospheric origin of the currents, and even current systems, that are observed in the photosphere. We therefore conclude that the currents responsible for sinuous coronal structures are of subphotospheric origin.

Subject headings: Sun: activity — Sun: corona — Sun: magnetic fields — Sun: X-rays, gamma rays — sunspots

1. INTRODUCTION

Observations made with the *Yohkoh* Soft X-Ray Telescope (SXT) have provided numerous examples of coronal structures with a sinuous forward or backward S shape (Acton et al. 1992). Canfield, Pevtsov, & Acton (1995) and Rust & Kumar (1996) interpreted these sinuous shapes as projections of helical structures, inferring the existence of current systems on active-region length scales. Such currents are not unexpected; ample evidence of strong active region–scale vertical currents at photospheric levels is provided by vector magnetograms of flare-producing active regions (e.g., Ding et al. 1987; Gary et al. 1987; Canfield et al. 1993). Although it has been argued that sheared coronal structures do not rule out potential fields (Priest & Milne 1980), it is not clear that the observed S-shaped structures within active regions can best be explained by potential fields.

In this paper we hypothesize that these coronal structures are twisted because of current systems of subphotospheric origin, which we observe as vertical currents (at photospheric levels) on their way into the corona. To test this hypothesis we compare values of the force-free field parameter α inferred from photospheric vector magnetograms to values determined from the geometries of associated coronal loops. We adopt the linear, or "constant-α," force-free field (e.g., Gary 1989) as our working model. We determine the single value of the parameter α that gives the best overall fit to the measured photospheric field, which we call α_p, or to the shape of the observed coronal field lines, which we call α_c. If the shear of coronal loops is determined by electric currents, we expect a strong correlation between α_p and α_c. On the other hand, if the shear is only apparent shear, not associated with coronal currents, then we expect no such correlation.

In the following sections we describe how we infer α in the photosphere from vector magnetograms (§ 2) and in the corona from X-ray images (§ 3). Section 4 presents the main result of the study—a close correlation in sign between $\langle \alpha_p \rangle$ and $\langle \alpha_c \rangle$.

2. PHOTOSPHERIC VECTOR MAGNETOGRAMS

To characterize active region–scale vertical currents at photospheric levels, we used vector magnetograms from the Haleakala Stokes Polarimeter (Mickey 1985) at Mees Solar Observatory. Our data set consisted of 655 photospheric magnetograms of 140 solar active regions obtained between 1991 November (after the *Yohkoh* spacecraft was launched) and 1995 May. The instrument has a 6″ circular aperture and scans the solar image to build up a vector magnetogram. We used the two standard types of vector magnetograms, half-resolution (step size 5″.6) and full-resolution (step size 2″.8), described by Canfield et al. (1993). The magnetograms were derived from Stokes profiles of the spectral lines Fe I $\lambda\lambda$ 6301.5 and 6302.5 using the nonlinear least-squares Unno profile fitting routine of Skumanich & Lites (1987). This method makes a first-order correction for magneto-optical and magnetic filling factor effects. The noise level in the original magnetograms was about ± 70 G for $B_{\rm trans}$ and ± 10 G for $B_{\rm long}$.

For each magnetogram we resolved the 180° azimuthal ambiguity of $B_{\rm trans}$, following Canfield et al. (1993). There is no reason to believe that the magnetic field at photospheric levels is force-free (e.g., Metcalf et al. 1995). Nevertheless, a useful way to characterize vertical currents on active region scales is to compute the value of α for a linear force-free field ($\nabla \times \boldsymbol{B} = \alpha \boldsymbol{B}$) that minimizes (in a least-squares sense) the difference between the horizontal components of the computed and observed fields, using only those pixels for which the vertical component $|B_{\rm vert}| > 100$ G. For active regions represented by several magnetograms, we used averages ($\langle \alpha_p \rangle$) of individual α_p values derived from single magnetograms.

3. CORONAL X-RAY IMAGES

To characterize α in the corona, we used the morphology of coronal loops observed in movies made from desaturated composite images from the *Yohkoh* SXT (Tsuneta et al. 1991). The interval between images was short enough (with respect to typical active region loop lifetimes) to allow us to identify most structures in a given active region. The composites of long and short exposures showed coronal structures over a wide range of intensity. We identified coronal loops that showed a distinctive forward or backward S shape, as illustrated in Figure 1.

Observations of active region–scale structures made over several days helped identify features of interest, although we determined α from individual frames near disk center, such as the one shown in the figure. We approximated the shape of such loops by a third-degree polynomial and determined the shear angle of this polynomial at the loop midpoint. It is clear that the value of α derived in this way can be distorted by projection effects. To minimize these effects we used only coronal loops close to the central meridian (typically within $\pm 20°$).

We focused on active region loops of length under 200″. We ignored the longer loops that interconnect active regions because there is ambiguity about the interpretation of such loops. In agreement with Priest & Milne (1980), Figure 2 shows that a simple potential-field model comprising a pair of offset dipoles can form distinctive S-shapes that have nothing to do with currents.

Since magnetic pressure exceeds gas pressure in the corona above solar active regions, magnetic fields there should be nearly force-free. Electric currents are then determined by $\mu_0 \boldsymbol{J} = \alpha \boldsymbol{B}$, where $\boldsymbol{J}$ is the current density, $\boldsymbol{B}$ is the magnetic induction, μ_0 is the permeability of free space, and α is constant along a field line.

Figure 3 shows model dipole force-free fields with $\alpha > 0$ and $\alpha < 0$. In projection onto the horizontal plane, the

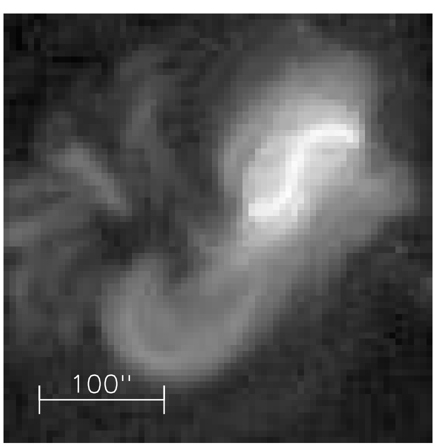

FIG. 1.—*Yohkoh* SXT image of a sheared coronal loop observed 1993 April 24 in AR 7480.

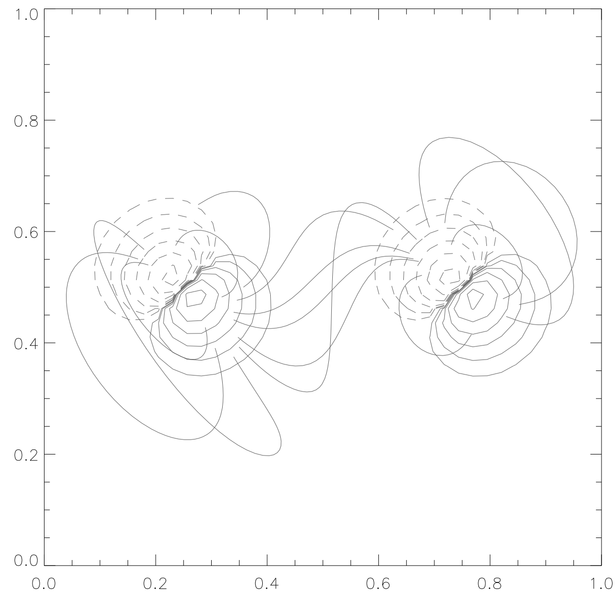

FIG. 2.—Magnetic potential field of an offset pair of dipoles. Contours show vertical magnetic field. Field lines connecting dipoles show distinctive forward-S shape, even though the magnetic field is current-free.

central magnetic field lines form a forward S for positive α and a backward S for negative α. Although the curvature of the field lines varies with position, the shear angle γ at the midpoint of the dipole is obviously related to α. Of course, any of the field lines shown in Figure 3 may happen to be outlined by bright coronal plasma. This results in an uncertainty in the observed value of γ that we estimate to be $\sim 10°$–$15°$.

Using photospheric vector magnetograms, we can in principle compute the coronal force-free field (e.g., Mikic & McClymont 1994) quite generally. In practice, that approach is far too demanding to apply to our large data set; we need a simplified approach that contains the essential characteristics necessary to test our hypothesis. It is sufficient to use a simple two-dimensional force-free field solution of separable form (e.g., Priest 1984). Suppose that a magnetic field has components in Cartesian coordinates (x, y, z),

$$B_x = -l/k\, B_0\, e^{-lz} \cos kx\,,$$
$$B_y = -(1 - l^2/k^2)^{1/2} B_0\, e^{-lz} \cos kx\,,$$
$$B_z = B_0\, e^{-lz} \sin kx\,, \tag{1}$$

where B_0 is the magnetic field strength on the axis of the loop ($x = z = 0$) and $L = \pi/k$ is the distance between foot-

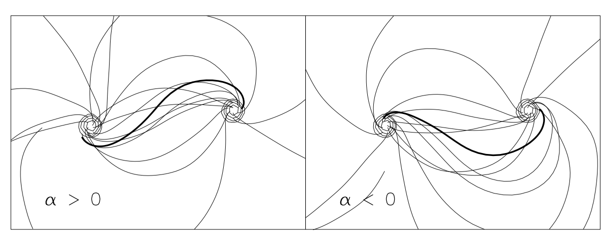

FIG. 3.—Model bipolar linear force-free fields computed for positive and negative α. Contours show vertical magnetic field strength. Magnetic field lines are projected onto the horizontal plane. A field line near the central part of the dipole is shown with a heavy line to demonstrate the sense of shear (i.e., forward S for positive α and backward S for negative α).

points. The constant-α solution has $\alpha = (k^2 - l^2)^{1/2}$ for this kind of field. In the horizontal (x, y)-plane, the angle γ between the field lines and the x-axis is

$$\gamma = \tan^{-1}\frac{B_y}{B_x} = \tan^{-1}\frac{\alpha L}{(\pi^2 - \alpha^2 L^2)^{1/2}}\,, \quad (2)$$

and thus

$$\alpha_c = (\pi/L)\sin\gamma\,. \quad (3)$$

A more general solution, valid for small α, which does not assume periodicity gives $\alpha_c \sim \tan\gamma$ (McClymont 1995). However, it is sufficient for the present purpose to use equation (3) to obtain α_c, since our goal is only to determine whether there is a correlation between $\langle\alpha_p\rangle$, obtained from photospheric magnetograms, and $\langle\alpha_c\rangle$, obtained from the shear angle of coronal loops.

4. CORRELATION BETWEEN PHOTOSPHERIC AND CORONAL α-VALUES

In the *Yohkoh* SXT data of 1991–1995, we identified 182 different loops showing measurable shear. During the same period of time roughly 1000 active regions were observed. Thus, the majority of coronal loops show little, if any, detectable shear. The minimum shear angle that we can measure is about 10°–15°. For $\gamma = 10°$ and $L = 150''$ (the average length of the 67 measured loops), equation (3) gives $\alpha_{\gamma=10} = 5 \times 10^{-9}\ \mathrm{m}^{-1}$ as the lower limit of detectability.

We were able to determine α_c values for only 67 of the 140 active regions for which we had vector magnetograms. Roughly half of the active regions in the vector magnetogram data set have $\langle\alpha_p\rangle$ less than $\alpha_{\gamma=10}$, so it is reasonable to expect that their α_c values are below our limit of measurement. Of course, sometimes the SXT spatial resolution was insufficient to resolve fine structure in the coronal loops. It is also possible that individual unresolved coronal loops seen in projection can mimic a single sheared loop. We avoided such cases, including in our study only those loops that exhibited unambiguous shear.

Of the 67 cases in which we measured both coronal and photospheric α values, 51 (76%) active regions had the same sign of α in the corona and photosphere and 16 (24%) had opposite signs. However, 23 of the 67 active regions had an $\langle\alpha_p\rangle$ value that was too small to produce the inferred value of $\langle\alpha_c\rangle$, i.e., $\alpha_p < \alpha_{\gamma=10}$. Excluding these cases, the remaining 44 active regions had the same sign of α in the photosphere and the corona in 39 cases (90%) and opposite sign in only five cases (10%). Such a high correlation between photospheric and coronal α implies a close connection between observed shear and electric current in these coronal loops. These results are summarized in Table 1.

Figure 4 shows a plot of $\langle\alpha_c\rangle$ versus $\langle\alpha_p\rangle$ for the 44 active regions that both showed pronounced shear of coronal loops and were not eliminated on account of small $\langle\alpha_p\rangle$ values. The uncertainties in coronal $\langle\alpha_c\rangle$ shown here are

TABLE 1

SIGN OF α_c AND α_p FOR 67 ACTIVE REGIONS

α_p Value	$\alpha_p\alpha_c > 0$	$\alpha_p\alpha_c < 0$	Total
$\lvert\alpha_p\rvert \geq \lvert\alpha_{\gamma=10}\rvert$	39	5	44
$\lvert\alpha_p\rvert < \lvert\alpha_{\gamma=10}\rvert$	12	11	23
Total	51	16	67

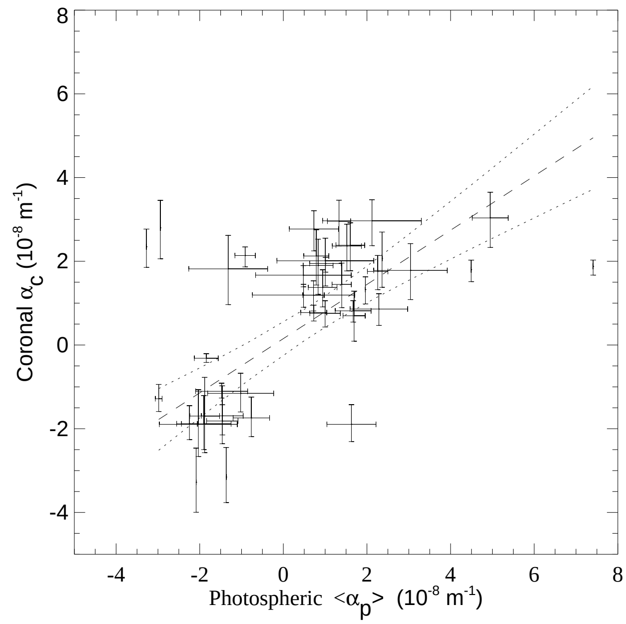

FIG. 4.—Observed force-free field parameter α from photospheric vector magnetograms ($\langle\alpha_p\rangle$) and from the geometry of coronal loops ($\langle\alpha_c\rangle$) for 44 active regions. Error bars are 1 σ for both parameters. Error bars for coronal $\langle\alpha_c\rangle$ correspond to 10° standard deviation in shear. Active regions for which only one magnetogram was taken are shown without error bars in $\langle\alpha_p\rangle$. The linear fit (*long-dashed line*) and 2 σ error band (*short-dashed lines*) are shown.

based on the uncertainties associated with the particular loop measured; the true standard deviation in $\langle\alpha_c\rangle$ may be higher, since different loops in a given active region have a range of values of shear.

In spite of the high correlation between the signs of $\langle\alpha_c\rangle$ and $\langle\alpha_p\rangle$, there are several active regions whose values of $\langle\alpha_c\rangle$ are clearly of sign opposite to $\langle\alpha_p\rangle$. How can we explain these? In the framework of this study we have treated photospheric and coronal magnetic fields as linear force-free fields. As noted above, α is quite variable over many active regions (see, e.g., Pevtsov, Canfield, & Metcalf 1994). For some of the active regions, the linear force-free field is a good approximation, but others require a nonlinear model. Using vector magnetograms, we may compute the vertical components of magnetic field (B_z) and current density (J_z) at every pixel (following Pevtsov et al. 1994). Figure 5 gives examples of both types of regions. Active Region 5747 (Fig. 5*a*) shows a good correlation between B_z and J_z. Such correlation suggests that the linear force-free field is a good approximation for this active region. AR 6919 (Fig. 5*b*), on the other hand, shows no correlation between B_z and J_z. Pevtsov et al. 1994 observed pronounced patches of both signs of α inside AR 6919.

If the force-free field is highly nonlinear, as in AR 6919, the linear approximation gives a value of $\langle\alpha_p\rangle$ that is much smaller in absolute value than (say) the rms value. Figure 6 shows another such region, AR 7123. The photospheric magnetogram (Fig. 6*a*) and α-map (Fig. 6*c*) show both signs of α in both the leading and the following polarities (see B and F symbols in Figs. 6*b* and 6*d*). The spatial resolution and accuracy of co-alignment between the photospheric (Fig. 6*a*) and the coronal images (Fig. 6*b*) are insufficient to determine exactly which patch of a given α value is related to which loop. However, it is obvious from the X-ray image

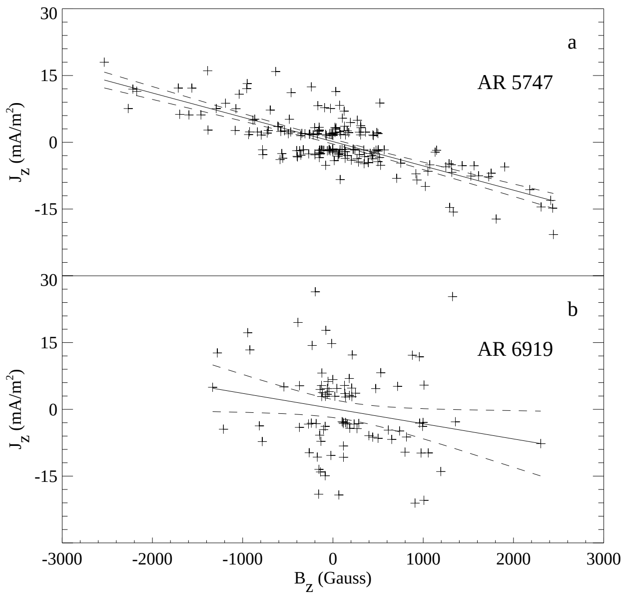

FIG. 5.—Observed density of the vertical electric current (J_z) as a function of vertical magnetic field (B_z) for active regions AR 5747 (*top*) and AR 6919 (*bottom*). The linear polynomial approximation and 2 σ error band (*dashed lines*) are shown.

in Figure 6*d* that both forward-S and backward-S loops are present. All of the 23 active regions that have a measured $\langle \alpha_c \rangle$ that is higher than expected from their $\langle \alpha_p \rangle$ have distinct patches of both signs of α. Although the existence of such a pattern of local α having opposite sign makes the correlation between $\langle \alpha_c \rangle$ and $\langle \alpha_p \rangle$ worse, indirectly it supports the concept that the shear of coronal loops is a signature of electric currents flowing along magnetic field lines.

5. CONCLUSION

Only about 20% of the active region coronal loops that we have studied in the *Yohkoh* data near disk center exhibit significant shear. However, nearly 50% of the 140 active regions for which we have vector magnetograms do so (magnetograms were made only for regions thought to be flare productive). Of these, 60% have the same sign of α in both the photosphere and the corona, while only 5% have $\langle \alpha_c \rangle$ and $\langle \alpha_p \rangle$ of opposite sign. The remaining 35% of active regions have average coronal shear exceeding the amount expected from their measured $\langle \alpha_p \rangle$. Half of these have $\langle \alpha_c \rangle$ and $\langle \alpha_p \rangle$ of the same sign and half have $\langle \alpha_c \rangle$ and $\langle \alpha_p \rangle$ of opposite sign.

The active regions that show either opposite signs of $\langle \alpha_p \rangle$ and $\langle \alpha_c \rangle$ or higher $\langle \alpha_c \rangle$ than expected from their $\langle \alpha_p \rangle$ also

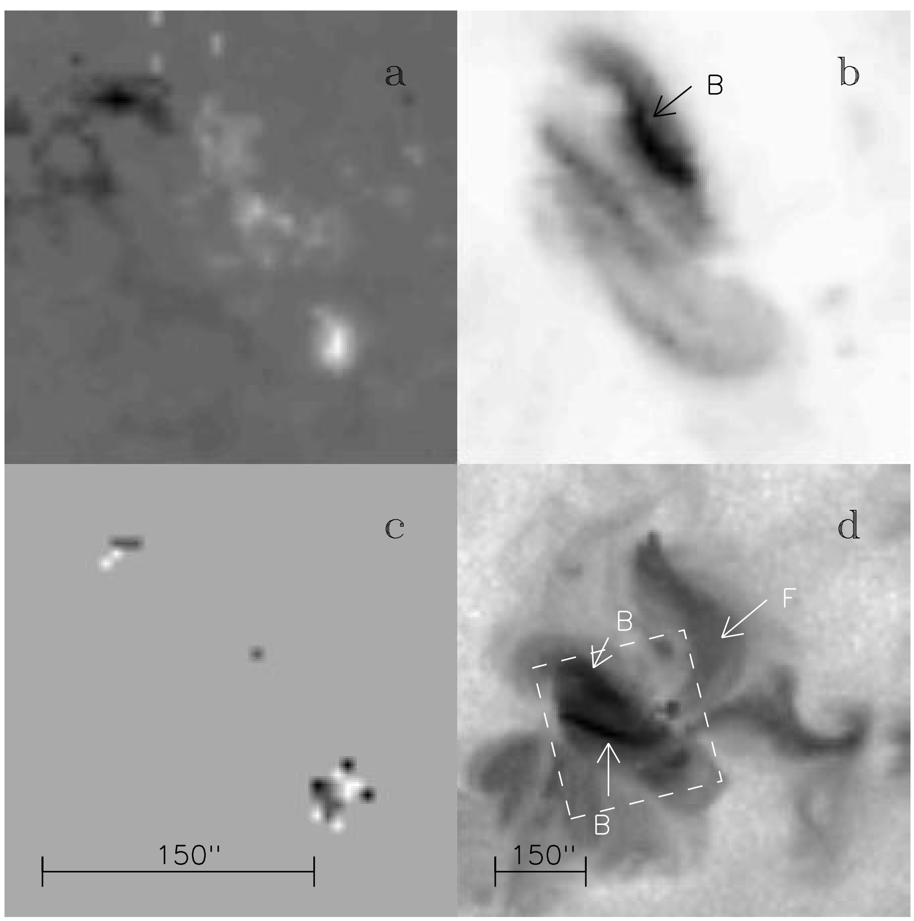

FIG. 6.—(*a*) Vertical magnetic field, (*b*, *d*) coronal loops, and (*c*) local values of $\alpha_z = J_z/B_z$ of AR 7123 on 1992 April 9. Positive magnetic field (*a*) and positive α_z (*c*) are shown in white. The uniform gray in (*c*) indicates pixels below the noise level in J_z and B_z. (*a*), (*b*), and (*c*) are co-aligned using centers of sunspots on white light images. The larger field of view in (*d*) shows the overall coronal structure of the active region. The white-dashed square in (*d*) indicates the size and position of the photospheric magnetogram in (*a*) and (*c*). The arrows show several backward (B) and forward (F) coronal loops.

tend to show patches of both signs of α in the photosphere. Numerous nonlinear averaging effects make the methods used in this paper of little value within such regions. Also, one must expect systematic effects because photospheric magnetic fields are not force-free, and our spatial resolution is high enough to resolve only large-scale variations. Hence one can not meaningfully compare the values of $\langle \alpha_p \rangle$ and $\langle \alpha_c \rangle$ directly in such cases.

For those active regions that are dominated by one sign of α in the photosphere, so that the $\langle \alpha_p \rangle$ determined by fitting a linear force-free field provides a good estimate of the magnitude of their photospheric currents on active-region scales, the close correlation between $\langle \alpha_c \rangle$ and $\langle \alpha_p \rangle$ clearly shows that the coronal currents extend down to the photosphere. However, it is important to ask whether they close in the photosphere or continue to significantly greater depth. As noted in the recent review by Low (1996), various lines of evidence lead to a picture of the Sun "... by which magnetic flux and helicity make their way from below the photosphere into the corona, and, ultimately, into interplanetary space." Lites et al. (1996) used a comprehensive set of polarimetric and imaging data made over the disk passage of an active region to conclude that they had observed the ascent of an entire magnetic system through the photosphere into the corona. Leka et al. (1996) used a different comprehensive set of both morphological and polarimetric data to show, by several independent methods, that new flux in an active region of notably vigorous emergence carried currents of subphotospheric origin. Furthermore, our recent work on the hemispheric and local structure of α in the photosphere (Pevtsov et al. 1994, 1995) and the amplitudes of J_z typically derived from solar vector magnetograms (McClymont, Jiao, & Mikic 1997) cannot plausibly be explained on the basis of local currents that close in the photosphere. We therefore must conclude that sinuous coronal loops indicate electric currents of subphotospheric origin.

We thank the staff of Mees Solar Observatory and the *Yohkoh* team for the observations. The *Yohkoh* Soft X-ray Telescope is a collaborative project of the Lockheed Palo Alto Research Laboratory, the National Astronomical Observatory of Japan, and the University of Tokyo, supported by NASA and ISAS. This investigation has been supported by National Science Foundation grants ATM 93-11937 and ATM 93-20575, NASA grants NAGW-1542 and NAGW-5072, and NASA contract NAS 8-37334.

REFERENCES

Acton, L. W., et al. 1992, Science, 258, 618
Canfield, R. C., et al. 1993, ApJ, 411, 362
Canfield, R. C., Pevtsov, A. A., & Acton, L. W. 1995, Eos, 76, S235
Ding, Y. J., Hong, Q. F., Hagyard, M. J., Deloach, A. C., & Liu, X. P. 1987, Sol. Phys., 109, 307
Gary, G. A. 1989, ApJS, 69, 323
Gary, G. A., Moore, R. L., Hagyard, M. J., & Haisch, B. J. 1987, ApJ, 314, 782
Leka, K. D., Canfield, R. C., McClymont, A. N., & van Driel-Gesztelyi, L. 1996, ApJ, 462, 547
Lites, B. W., Low, B. C., Martinez Pillet, V., Seagraves, P., Skumanich, A., Frank, Z. A., Shine, R. A., & Tsuneta, S. 1996, ApJ, 446, 877
Low, B. C. 1996, Sol. Phys., 167, 217
McClymont, A. N. 1995, unpublished
McClymont, A. N., Jiao, L., & Mikic, Z. 1997, Sol. Phys., in press
Metcalf, T. R., Jiao, L., McClymont, A. N., & Canfield, R. C. 1995, ApJ, 439, 474
Mickey, D. L. 1985, Sol. Phys., 97, 223
Mikic, Z., & McClymont, A. N. 1994, in ASP Conf. Proc. 68, Solar Active Region Evolution: Comparing Models with Observations, ed. K. S. Balasubramaniam & G. Simon (San Francisco: ASP), 225
Pevtsov, A. A., Canfield, R. C., & Metcalf, T. R. 1994, ApJ, 425, L117
———. 1995, ApJ, 440, L109
Priest, E. R. 1984, Solar Magnetohydrodynamics (Dordrecht: Reidel)
Priest, E. R., & Milne, A. N. 1980, Sol. Phys., 65, 315
Rust, D. M., & Kumar, A. 1996, ApJ, 464, L199
Skumanich, A., & Lites, B. W. 1987, ApJ, 322, 473
Tsuneta, S., et al. 1991, Sol. Phys., 136, 37